IEEE Access
Multidisciplinary | Rapid Review | Open Access Journal

Received October 12, 2021, accepted October 20, 2021, date of publication October 26, 2021, date of current version November 2, 2021.

Digital Object Identifier 10.1109/ACCESS.2021.3123253

Antenna Decoupling Based on Self-Resonance Frequencies of Common Mode and Differential Mode

ANPING ZHAO, (Senior Member, IEEE), AND ZHOUYOU REN, (Member, IEEE)
Huami Information Technology Company Ltd., Shenzhen 518000, China
Corresponding author: Zhouyou Ren (renzhouyou@zepp.com)

ABSTRACT This article presents a simple and effective decoupling approach based on the common mode (CM) and differential mode (DM) analysis to solve decoupling problem between two symmetrical antenna elements. Especially, the concept of the self-resonance frequencies of CM and DM is utilized in antenna decoupling analysis. It is found that when the self-resonance frequencies of CM and DM are the same, strong mutual coupling between two symmetrically and closely placed two-port antennas can be completely eliminated. The difference between self-resonance frequency and resonance frequency is discussed; and the method of obtaining the self-resonance frequencies of CM and DM is given. Since the proposed antenna decoupling judgment condition is straightforward and simple, it can effectively deal with any kind of closely placed antenna system with a plane of symmetry; and obtain good decoupling effect simply and easily. The effectiveness, feasibility and advantage of the proposed decoupling condition for the CM and DM analysis are demonstrated through several symmetrical two-port antenna examples. The decoupling approach proposed in this article can undoubtedly make the common mode and differential mode analysis for solving antenna decoupling problems more effective and practical.

INDEX TERMS Antenna decoupling, common and differential modes analysis, coupled resonator, equivalent circuit of antenna system, self-resonance frequency.

I. INTRODUCTION

How to effectively reduce the mutual coupling in antenna array or multiple-input and multiple-output (MIMO) antenna system has always been a difficult problem, especially when the antennas are placed very close to each other. To solve this problem, several decoupling techniques or methods for reducing the antenna isolation have been proposed, e.g., by using neutralization line [1]–[4], decoupling network [5]–[7], dual-polarization [8], [9], pattern diversity [10], multimode decoupling technique [11], self-curing method [12], self-decoupled method [13]–[16], high-order mode [17], electromagnetic bandgap [18], defected ground structure [19]–[21], hybrid electric and magnetic coupling method [22], metasurface-based decoupling technique [23], and common mode and differential mode analysis [24]–[27]. It can be noticed that most antenna structures [1]–[27] have the following common features: two antenna elements are symmetrically and closely placed. Because of the above arrangement, these antenna systems undoubtedly lead to very strong coupling between the two antennas, so how to achieve good decoupling or isolation is a rather challenging task.

Recently, the common mode (CM) and differential mode (DM) analysis has been successfully applied to the antenna decoupling problems [24]–[27]. In particular, the concept of mode-cancellation analysis based on CM and DM was proposed in [25]–[27], which perfectly reveals that the decoupling mechanism (in terms of electromagnetic field) of two symmetrically and closely placed antennas can be elaborated by superimposing the current distributions of CM and DM. In addition, to achieve decoupling condition, the two-port antenna system was analyzed with the scattering parameter method [25]–[27]. And, it was found that the isolation between two antennas can be equivalent to the difference between the complex or active reflection coefficients (or impedances) of CM and DM. Although it was claimed [25]–[27] that such a decoupling condition could be obtained by comparing the Euclidean distance of CM and DM in Smith chart within the frequency range of interest, the comparison process is still quite complicated or at least

The associate editor coordinating the review of this manuscript and approving it for publication was Pavlos I. Lazaridis.

not straightforward, especially when the form of the active or complex impedances (i.e., the impedance curves in Smith chart) of CM and DM appears very differently (e.g., not overlapped each other) in Smith chart; and unfortunately, this may exist in most two-port antenna systems.

Since an antenna system can be analyzed by either the scattering parameter method [25]–[27], [32] or the equivalent circuit model [14]. Therefore, to overcome the above shortcomings, a simple and effective decoupling approach is proposed for general symmetrically and closely placed two-port antenna systems. In particular, the two-port antenna system is analyzed by using the equivalent circuit of the system. It is found that when the self-resonance frequencies of CM and DM are identical, perfect antenna decoupling can be obtained. In fact, the derivation of the above-mentioned decoupling condition is inspired by the design of coupled resonant filters [28]–[30]. Through a comparative analysis, we found that the strong coupling exists in both the coupled resonator system and symmetrically and tightly placed two-port antenna system; and the intrinsic relationship between the two systems on the coupling was obtained. In addition, due to the symmetry, both the systems can be analyzed by CM and DM analysis. On the other hand, although the existence of strong coupling is expected in coupled resonator systems, when the coupling coefficient of the system is zero the strong coupling will disappear completely. Even though the above zero coupling condition is not a design goal at all in filter designs, this zero coupling condition is exactly the goal pursued by the antenna decoupling design.

This article is organized as follows. In Section II, the basic theory of coupled resonant filter is introduced and the decoupling condition for CM and DM analysis is derived. In Section III, the advantage and effectiveness of the proposed decoupling condition are verified through several examples. In Section IV, some specific issues related to the proposed approach are discussed. Finally, the conclusion of this work is given in Section V.

II. THEORY

In this section, the equivalent circuit of a coupled resonator filter is presented and the mixed coupling coefficient of the coupled resonator is derived. Then, the equivalence between the coupled resonator and symmetrically and closely placed two-port antenna systems is discussed. The decoupling condition based on the self-resonance frequency of CM and DM for achieving good antenna decoupling is presented. The ways to obtain the active or complex impedances of CM and DM are given. Finally, the main difference in decoupling conditions between the proposed method and the one developed in [25]–[27] is briefly discussed.

A. EQUIVALENT CIRCUIT OF COUPLED RESONATOR

Fig.1 shows the equivalent circuit of a symmetrically placed coupled resonator filter with a coupling reactance M. Each

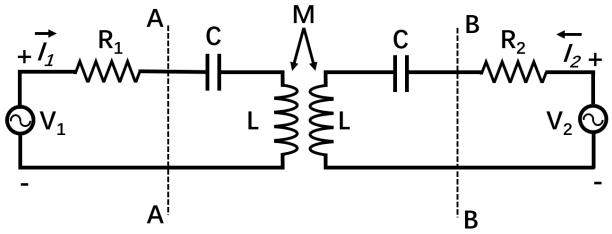

FIGURE 1. Equivalent circuit of a coupled resonator (or a two-port antenna system) with coupling reactance M.

uncoupled resonator is composed of a capacitance C and an inductance L and is characterized by its self-resonance angular frequency $\omega = (LC)^{-1/2}$ [28], [29]. For this symmetrical two-port system, $R_1 = R_2 = R$ is the equivalent resistor and V_1 and V_2 are respectively the source voltage of the ports. According to the equivalent-circuit theory, if the reference planes A-A and B-B in Fig. 1 are open circuited, then an equivalent transformed circuit shown in Fig. 2 can be derived [28], [29], in which S-S is the symmetrical plane and C_m and L_m are the mutual inductance and mutual capacitance of the coupled resonator. Generally speaking, there is a mixed coupling in the coupled resonator. And, this mixed coupling can be divided into electric coupling and magnetic coupling when an electric wall (or a short-circuit) or a magnetic wall (or an open-circuit) is separately inserted at the symmetrical plane. Due to the characteristics of the open- and short-circuit, the coupling of the coupled resonator can be divided into two modes: the common mode (CM) (related to the magnetic wall) and the differential mode (DM) (related to the electric wall) when the magnetic and electric walls are respectively applied. In addition, the capacitance C_m leads to the electric coupling of the coupled resonator, whereas the inductance L_m results in the magnetic coupling [28], [29]. When the electric and magnetic walls are applied separately to the symmetrical plane S-S, the equivalent transformed

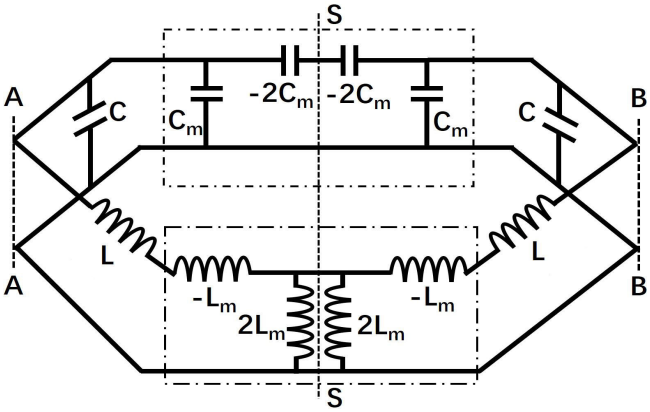

FIGURE 2. Associated equivalent transformed circuit of a coupled resonator circuit (or coupling part of symmetrical two-port antenna system) with mixed coupling, where Cm and Lm are related to electric coupling and magnetic coupling, respectively.

circuit in Fig. 2 results in the following self-resonance frequencies [28], [29]:

$$f_{CM} = \frac{1}{2\pi\sqrt{(L - L_m)(C - C_m)}} \quad (1)$$

$$f_{DM} = \frac{1}{2\pi\sqrt{(L + L_m)(C + C_m)}} \quad (2)$$

where f_{CM} and f_{DM} are respectively the self-resonance frequencies of the CM and DM of the coupled resonator. The reason why f_{CM} and f_{DM} are called the self-resonance frequencies [28], [29] is that f_{CM} and f_{DM} vary only with the intrinsic parameters, i.e., the inductances (L and L_m) and capacitances (C and C_m) of the coupled resonator system itself. Hence, the self-resonance frequencies can also be seen as the inherent characteristics of the coupled resonator system. Certainly, the values of f_{CM} and f_{DM} can be calculated once L, L_m, C, and C_m are known. However, these values, especially L_m and C_m, are usually not directly known. Nevertheless, we found that without knowing these values, if an excitation port is applied to the reference plane A-A or B-B, f_{CM} and f_{DM} can still be obtained. The reason why the self-resonance frequency can be obtained by applying an excitation port to the reference plane A-A or B-B will be discussed in detail in Section IV.

From Eqs. (1-2), the mixed coupling coefficient of the coupled resonator can be obtained as [28], [29]:

$$K_x = \frac{f_{CM}^2 - f_{DM}^2}{f_{CM}^2 + f_{DM}^2} \quad (3)$$

Obviously, the mixed coupling coefficient, K_x, varies simultaneously with L_m and C_m. Note that a formula that has the same meaning (using ω instead of f) as Eq. (3) can be obtained for the coupled resonator even a different equivalent circuit was adopted [30] (CM and DM are called even mode and odd mode in [30], respectively). This means that Eq. (3) is a general formula for any type of coupled resonator system. One can see from Eq. (3) that the mixed coupling coefficient of the coupled resonator will be zero if $f_{CM} = f_{DM}$. In fact, the zero mixed coupling coefficient is equivalent to that the electric coupling and magnetic coupling of the coupled resonator being balanced or cancelled. Although the zero mixed coupling coefficient is not the goal of filter design, we found that this feature can be perfectly utilized in the antenna decoupling design of any type of symmetrical two-port antenna system.

B. EQUIVALENCE BETWEEN COUPLED RESONATOR AND CLOSELY PLACED TWO-PORT ANTENNA SYSTEM

Generally speaking, there is always strong coupling in all symmetrically and closely placed two-port antenna systems, as the two antennas of the system are often placed very close to each other. Such a strong coupling is very similar to that of the coupled resonator. In addition, there are many other similarities between the closely placed two-port antenna system and the coupled resonator system. For example, they both have two ports; and most importantly, by applying a magnetic wall and an electric wall to the plane of symmetry, they can both be discretized into the CM and DM [26]–[30]. The above characteristics of course mean that the two systems can be equivalent from the perspective of coupling. In other words, under a condition when the mixed coupling of the system is changed from strong (coupled resonator) to weak (decoupled antenna), the equivalent circuit and the mixed coupling effect of the two-port antenna system can be represented, respectively, by the equivalent circuits of the coupled resonator shown in Fig. 1 and Fig. 2. Under the above condition, the coupling coefficient of the symmetrically and closely placed two-port antenna system can also be represented by Eq. (3). However, in the case of decoupled antenna, a smaller value (rather than a larger value in the case of coupled resonator) of K_x is pursued. Moreover, the self-resonance frequencies of the CM and DM of the symmetrical two-port antenna system can also be represented by f_{CM} and f_{DM} of Eq. (1) and Eq. (2).

Due to the above equivalences, when the mixed coupling coefficient is equal or close to zero, the coupling mechanism in the coupled resonator system can be used to decouple the symmetrically and closely placed two-port antenna system. Therefore, when the self-resonance frequencies of CM and DM of the two-port antenna system are identical (i.e., $f_{CM} = f_{DM}$), the strong coupling of the two-port antenna system can be totally eliminated, as in this case $K_x = 0$. This also means that in this case the electric coupling and the magnetic coupling are balanced and thus can cancel each other out. If the electric and magnetic couplings are unbalanced, then a complete (or partial) additional decoupling structure needs to be inserted into the two-port antenna systems; especially when the two antennas are not placed very close to each other. For example, to obtain good decoupling effect in the two-dipole antenna system, a complete additional decoupling structure was adopted [26]. The purpose of inserting the decoupling structure is to balance the electric coupling and magnetic coupling of the antenna system; and the better the balance, the better the decoupling effect.

To judge whether a good decoupling effect of the two-port antenna system is achieved, one can directly compare the difference between the self-resonance frequencies of CM and DM, rather than comparing the active reflection coefficients or impedances of CM and DM in Smith chart [25]–[27]. In order to more accurately and effectively reflect the difference for the self-resonance frequencies of CM and DM, we define the relative frequency difference, RFD, as:

$$\text{RFD} = \frac{|f_{CM} - f_{DM}|}{(f_{CM} + f_{DM})/2} \quad (4)$$

where f_{CM} and f_{DM} are the self-resonance frequencies of CM and DM, respectively. Of course, the degree of the decoupling effect of the two-port antenna system can also be validated by the value of the mixed coupling coefficient, K_x. The small the value of RFD (or K_x), the better the decoupling effect; and once the value of RFD (or K_x) is zero, perfect decoupling is achieved.

On the other hand, it should be mentioned here that since the very extreme condition (i.e., K_x is equal or very close to zero) of the coupled resonator is used for the decoupling of the two-port antenna system, and the RFD value can be calculated once the values of f_{CM} and f_{DM} are known. In addition, it should be noted that in order to calculate the RFD value, the values of f_{CM} and f_{DM} should coexist within the frequency range of interest. Otherwise, a smaller value of RFD can never be obtained. Therefore, as a prerequisite for obtaining optimal decoupling, same number of self-resonance frequencies of CM and DM should exist within the frequency range of interest. The above number can be equal to or greater than one; and when it is greater than one, such as two, better decoupling can be achieved. In fact, this phenomenon is very similar (but the purpose is opposite) to the high-order filter [28]–[30]. In the filter design, the higher the order, the better the filter performance. In contrast, however, in the case of antenna design, higher order leads to better decoupling effect. Moreover, when the number is greater than one, we need to calculate the RFD value for each group of CM and DM separately, and then take the average value as the final RFD value. Note that in the filter design, a calculation method similar to the above was also used when dealing with the high-order cases [30].

It should be emphasized here that although there are some differences between the coupled resonator filter and antennas, e.g., in general antenna radiates but filter doesn't, the coupling mechanism between them are the same: the coupling existing in both the coupled resonator filter and symmetrical two-port antenna can always be divided into electric coupling (related to DM) and magnetic coupling (related to CM) [28]–[31]. The only difference is that the coupling should be maximized in filter design, while the coupling should be minimized in antenna design. In particular, since the electric and magnetic couplings have opposite signs [28]–[31], when the total coupling coefficient (i.e., the sum of the electric and magnetic couplings) is equal or very close to zero, antenna decoupling can be achieved [31]. In fact, the CM and DM analysis was originally proposed and used for the coupled resonator filter designs [28]–[30]; and later it was extended and applied to the antenna decoupling problems [26], [27], [31]. This also means that two different systems (coupled resonator filter and symmetrical two-port antenna system) can both be designed through the same CM and DM analysis, which course indicates that there is a very close relationship between the coupled resonator filter and symmetrical two-port antenna system. Hence, it is precisely because of the existence of the above-mentioned close relationship that we can deduce the decoupling condition of the antenna system from the coupled resonator.

C. DIFFERENCE BETWEEN SELF-RESONANCE FREQUENCY AND RESONANCE FREQUENCY

It is worth mentioning here that the self-resonance frequency of an antenna is usually different from the frequency associated with the notch (or deepest point) in its S_{11} curve.

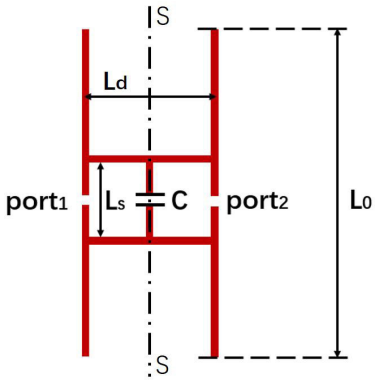

FIGURE 3. Geometry of a two-dipole antenna system similar to one proposed in [26]; and S-S is the symmetrical plane of the system.

The frequency associated with the notch is often called the resonance (or working) frequency of the antenna. This is also the frequency that antenna designers are interested in, because at this frequency, the total efficiency of the antenna is higher. But, the self-resonance frequency of an antenna corresponds to the frequency where the imaginary part of the antenna input impedance is zero. In fact, the self-resonance frequency and the resonance frequency of an antenna can also be distinguished in Smith chart. For example, the self-resonance frequency in Smith chart refers to the frequency at which the impedance curve intersects the real axis. On the contrary, the resonance frequency corresponding to the notch in S_{11} curve is equal to the frequency at the minimal distance from the center of Smith chart. Although the resonance frequency and the self-resonance frequency of an antenna are usually different, they can still be the same under certain special conditions, e.g., when the impedance curve in Smith chart is symmetrical along the real axis. Due to the above differences, it should be ensured that the self-resonance frequencies of CM and DM, rather than the resonance frequencies, are used when calculating the RFD value. The importance of using the self-resonance frequency to calculate the RFD value will be discussed in Section IV.

D. WAYS TO OBTAIN THE ACTIVE OR COMPLEX IMPEDANCES OF CM AND DM

The impedances or reflection coefficients (which can be called as the complex or active ones in general) of the CM and DM can actually be obtained/simulated with two different ways: (1) exciting only one of the two ports and applying the electric wall (i.e., PEC wall) or the magnetic wall (i.e., PMC wall) to the symmetrical plane S-S of the antenna system (see Fig. 3); in this case the impedance of CM is obtained while the PMC wall is applied, whereas the impedance of DM is obtained while the PEC wall is adopted. (2) exciting the two ports simultaneously with different phases [26]; in this case the impedance of CM is obtained when the two ports are excited in-phase (i.e., with 0-degree phase difference), whereas the impedance of DM is obtained when the two ports are excited out-of-phase (i.e., with 180-degree phase

difference). Because applying the PMC (PEC) wall to the symmetrical plane of an antenna system is equivalent to using in-phase (out-of-phase) excitation to excite the two-port antenna system, so the impedances of the CM or DM obtained with the above two ways are exactly the same; and the first way is adopted for all the examples considered in this article. In addition, the active impedances of CM and DM can also be calculated from the complex form of S_{11} and S_{21} as described in [26].

E. MAIN DIFFERENCE IN DECOUPLING CONDITION BETWEEN THE PROPOSED METHOD AND THE ONE DEVELOPED IN [25]–[27]

The main difference between the proposed decoupling method and the one developed in [25]–[27] is the different conditions used to evaluate the decoupling. In [25]–[27], decoupling is evaluated by comparing the difference/similarity between the complex (or active) impedances of CM and DM, specifically it is done by comparing the difference between the impedance curves of CM and DM in a certain frequency range in the Smith chart. Of course, when the impedance curves of CM and DM in the Smith chart are very similar or overlapped, the above comparison can be easily made. However, in most cases, the impedance curves of CM and DM in the Smith chart behave very differently, which will bring difficulties to the evaluation of decoupling. However, on the contrary, in the proposed method, the decoupling is evaluated by comparing the complex impedance of CM and DM at the self-resonant frequency; in particular, the detailed degree of decoupling can be evaluated by simply comparing the RFD value of CM and DM. Therefore, whether or not the impedance curves of CM and DM in the Smith chart are similar, the decoupling can always be easily evaluated by calculating the RFD value at the self-resonant frequency of CM and DM. It should be pointed out here that in the above two decoupling methods, the (active or complex) impedances of CM and DM used for decoupling evaluation are the same. In fact, the difference in decoupling conditions between the two decoupling methods is caused by the different ways of handling the antenna system. In this article, the antenna system is analyzed through the equivalent circuit model, but in [25]–[27] the antenna system is handled by the scattering parameter model. The superiority of the decoupling condition proposed in this article will be explained and demonstrated in the following sections.

III. VALIDATIONS

In this section, three typical decoupled two-port antenna systems [15], [26] will be used to verify the proposed decoupling approach. In addition, each of the two-port antenna systems has its own symmetrical plane, which ensures that CM and DM analysis can be applied to those antenna systems. Note that in this section the verification will be focused only on the proposed decoupling condition, since the comparison between simulation and measurement results (including total efficiency and ECC of examples 2 and 3) considered here were performed and confirmed in [15], [26].

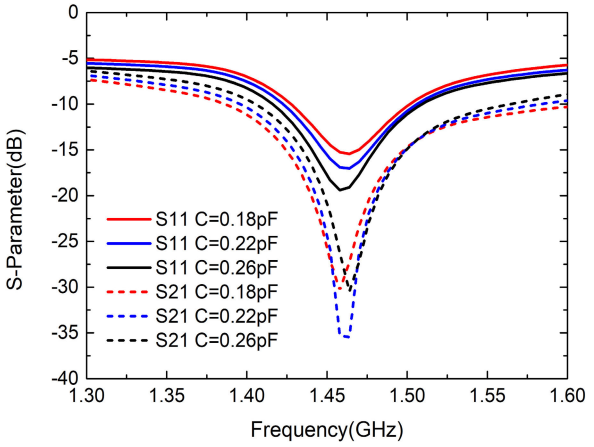

FIGURE 4. S-parameters of the antenna system varying with capacitor, C.

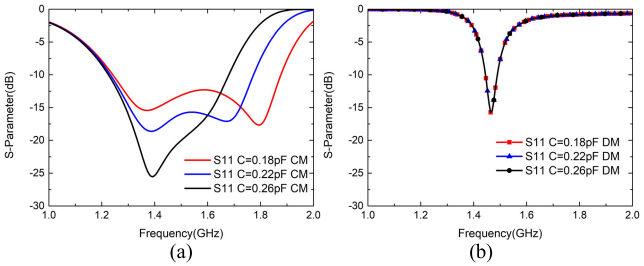

FIGURE 5. Simulated S11 of two-dipole antenna system varying with capacitor, C. (a) CM; (b) DM.

Example 1 (Two-Dipole Antenna System): The first example used for the validation is the two-dipole antenna system [26], as shown in Fig. 3; and S-S is the symmetrical plane of the system. In order to understand the characteristics of the antenna system more extensively, some dimensions of the dipole system used here are slightly different from those used in [26]. In particular, $L_0 = 100$mm, $L_d = 40$mm and $L_s = 20$mm are used in the simulation; and the areas of the cross section of dipoles and the strips are 1mm^2. As demonstrated in [26], the isolation between the two dipoles can be optimized when a decoupling structure is established by inserting some horizontal and vertical strips, and a lumped capacitor (C) in the middle of the vertical strip. And, the decoupling structure plays an important role in balancing the electric coupling and the magnetic coupling of the antenna system. Fig. 4 shows the S-parameter of the antenna system varying with different values of C. It can be seen from Fig. 4 that optimal isolation is obtained when C = 0.22pF. We will prove that the above optimal value of C can be easily obtained with the proposed decoupling approach.

Figs. 5(a) and 5(b) illustrate S_{11} of CM and DM varying as a function of C, respectively. It can be seen from Figs. 5(a) and 5(b) that S_{11} of the CM varies greatly with the value of C; and there is a double resonance (represented by the two notches) mode. In contrast, for the DM shown

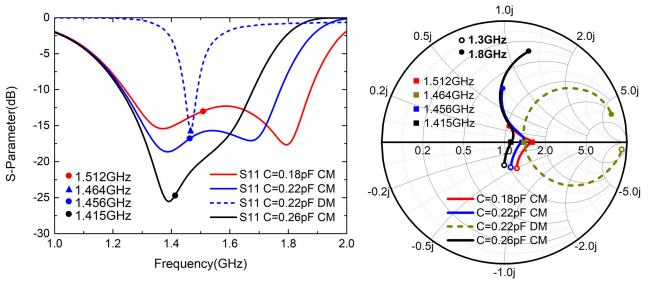

FIGURE 6. Comparison of CM and DM of a two-dipole antenna system with different values of capacitor. (a) S11; (b) Smith chart. Markers represent the self-resonance frequencies of CM and DM.

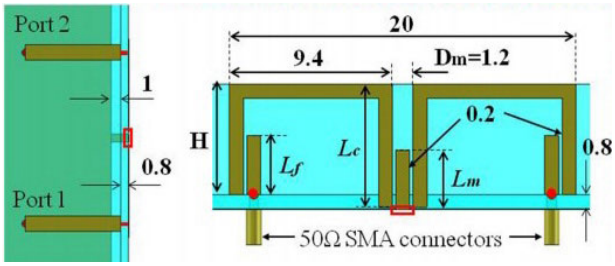

FIGURE 7. Geometry of a compact decoupled antenna pair [15] with a decoupled element (height Lm). All dimensions are in mm.

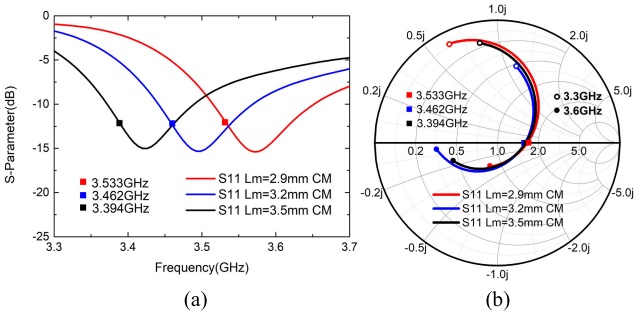

FIGURE 8. Simulated (a) S11 and (b) Smith chart of CM varying with Lm. Markers represent the self-resonance frequencies of CM.

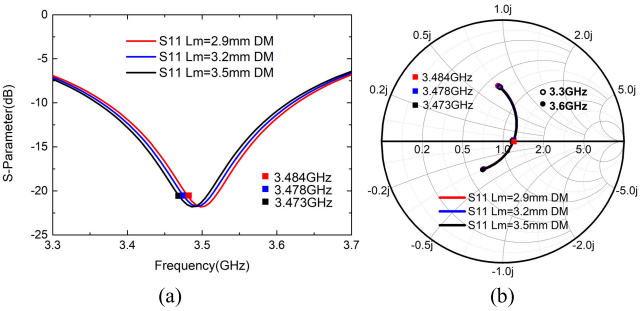

FIGURE 9. Simulated (a) S11 and (b) Smith chart of DM varying with Lm. Markers represent the self-resonance frequencies of DM.

in Fig. 5(b), it is almost unchanged while C varies, and only a single resonance mode exists. For comparison, the impedances of the CM and DM in S_{11} and Smith chart are plotted in Figs. 6(a) and Fig. 6(b), respectively. The markers represent the self-resonance frequencies of the CM and DM, which are determined in Smith chart by the frequencies corresponding to the intersections of the impedance curves and the real axis. This is because, as stated in Section II, the imaginary part of the impedance at these intersections is zero. Note that, as the variation of the DM with different values of C is ignorable, so only one curve for the DM (with C = 0.22pF) is drawn in Figs. 6(a) and 6(b). It can be seen from Fig. 6(a) that in this case the self-resonance frequencies and the resonance frequencies (related to the notches in S_{11} curves) of the CM and DM are not the same. In order to obtain the optimal value of C for decoupling, the RFD values of C = 0.18pF, 0.22pF and 0.26pF, which are calculated by Eq. (4) from the self-resonance frequencies shown in Fig. 6, are 3.23%, 0.55%, and 3.40%, respectively. This means that for this dipole antenna system the best isolation can be obtained while the value of C is at its optimal value of 0.22pF. Obviously, the above conclusion can be proven from the curves shown in Fig. 4. However, if one wants to compare the impedance difference between the CM and DM in either Smith chart or S_{11} curve, it would be difficult to find this optimal capacitance value because there is almost no any similarity between the impedance curves of CM and DM within the frequency range of interest. Instead, the optimal capacitance value can be simply found with the proposed decoupling approach, i.e., by directly comparing the RFD values of CM and DM. The above certainly confirms the usefulness and feasibility of the proposed decoupling approach.

Example 2 (Compact Decoupled Antenna Pair): The second example used for the validation is the antenna system with compact decoupled pairs proposed in [15], and the bottom and side views of the compact decoupled pair are shown in Fig. 7. It was demonstrated [15] that the height (L_m) of the decoupled element (i.e., the common grounding branch) located in the center of the antenna pair is a key parameter for achieving good isolation. Because in this antenna system the two antennas are placed very close to each other, so the balance between the electric coupling and the magnetic coupling can be achieved by inserting this simple decoupled element. Due to the symmetry, both CM and DM of this antenna system exist. Figs. 8(a) and 8(b) show S_{11} and Smith chart of CM as a function of L_m, respectively; whereas S_{11} and Smith chart of DM varying with L_m are illustrated in Figs. 9(a) and 9(b). Similarly, markers represent the self-resonance frequencies of CM and DM. It can be seen from Figs. 8 and 9 that although the impedance of DM changes slightly with L_m, a large variation for CM is observed.

The RFD values corresponding to L_m = 2.9mm, 3.2mm, and 3.5mm are 2.30%, 0.72% and 1.40%, respectively; and the best decoupling effect is achieved when L_m = 3.2mm. This can be simply proven by the S-parameters of the compact decoupled antenna system varying with L_m, as shown in Fig. 10. Figs. 11(a) and 11(b) show the comparison of CM and DM in S_{11} and Smith chart, respectively. It can be seen from Fig. 11(b) that without using the proposed

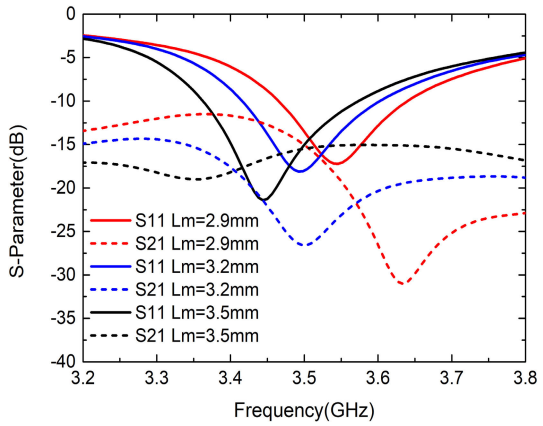

FIGURE 10. Simulated S-parameters of compact antenna system varying with Lm.

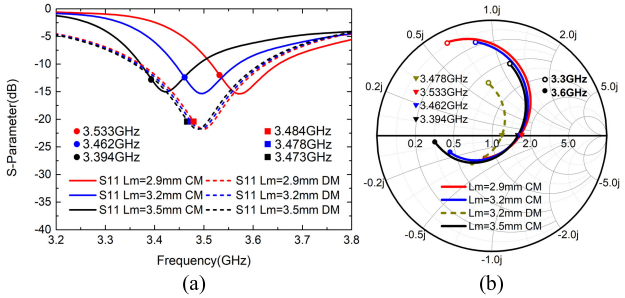

FIGURE 11. Comparison of CM and DM with different values of Lm. (a) S11 and (b) Smith chart. Markers represent the self-resonance frequencies of CM and DM.

decoupling approach, it is still quite difficult to distinguish in Smith chart which value of L_m could be optimal for the best decoupling, as within the frequency range of interest the impedance curves of CM and DM do not have good similarity. The above example once again demonstrates the usefulness and advantage of the proposed decoupling approach.

Example 3 (Closely Spaced Magnetic-Type Antenna System): The last example used for the validation is the closely spaced magnetic-type antennas (PIFAs) antenna system [26]; the three cases (i.e., with different sizes of the ground plane [26]), as shown in Fig. 12, will be considered. In this example, no any extra decoupling structure is needed, as the electric coupling and the magnetic coupling are balanced by the antenna structure itself; and the size of the ground plane plays a very important role in the balance.

Figs.13(a) and 13(b) respectively illustrate S_{11} and Smith chart of CM for the three cases; whereas for DM they are shown in Figs. 14(a) and 14(b). Markers in Figs. 13 and 14 represent the self-resonance frequencies of CM and DM. One can see from Figs. 13 and 14 that, except for CM of case 1, all other cases (including CM and DM of cases 2 and 3, and DM of case 1) have two self-resonance frequencies within the frequency range of interest (i.e., 1.3-1.7GHz).

The S-parameters of the antenna system with the three different cases are shown in Fig. 15. It can be seen from Fig. 15

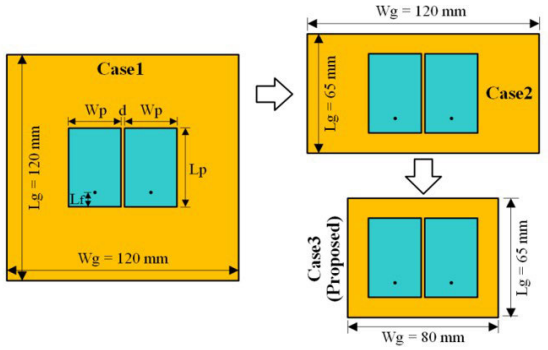

FIGURE 12. Three cases of magnetic-type PIFA antenna system proposed in [26].

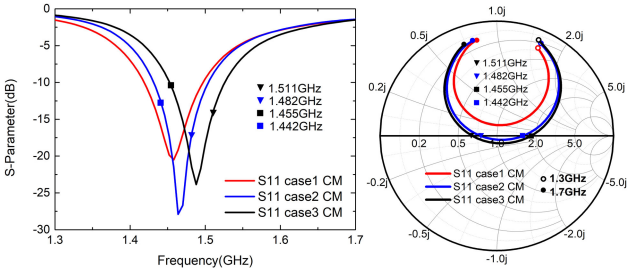

FIGURE 13. Simulated (a) S11 and (b) Smith chart of CM for three cases. Markers represent the self-resonance frequencies of CM.

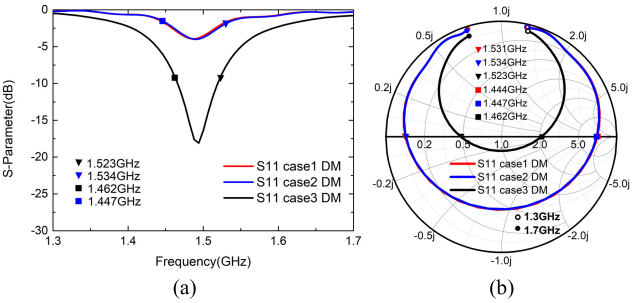

FIGURE 14. Simulated (a) S11 and (b) Smith chart of DM for three cases. Markers represent the self-resonance frequencies of DM.

that among the three cases quite poor isolation is obtained for case 1. The reason for this poor isolation is that in case 1 the self-resonance frequency, within the frequency range of interest, only appears in DM. In other words, the self-resonance frequency in the CM doesn't exist, as within the frequency range of interest the impedance curve of the CM doesn't have any intersections with the real axis in Smith chart. This of course indicates that for case 1 the precondition for achieving optimal decoupling cannot be met. Therefore, good isolation for case 1 cannot be achieved within the frequency range of interest. Moreover, it should be noted here that the absence of the self-resonance frequency for the CM just means that there is no self-resonance frequency within the frequency range of interest, not that the CM itself doesn't have a self-resonance frequency. In fact, the self-resonance frequency of the CM

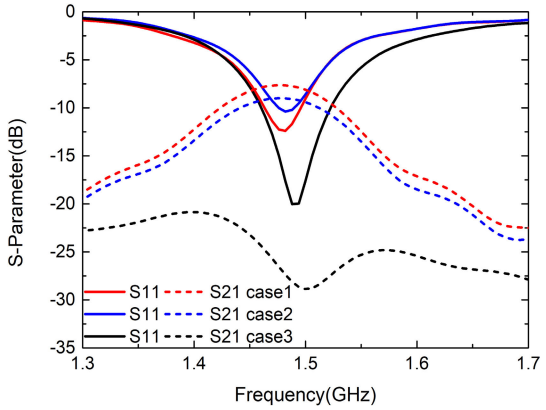

FIGURE 15. Simulated S-parameters of magnetic-type antenna system for three different cases.

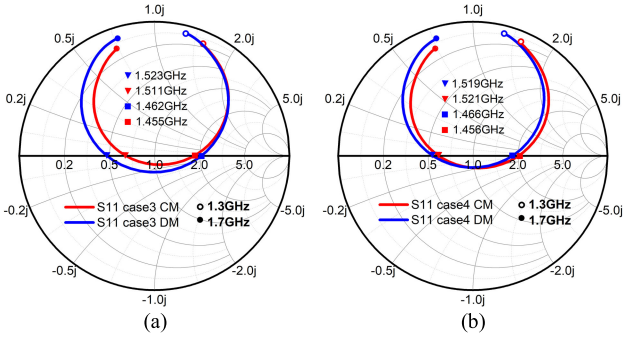

FIGURE 16. Comparison of impedance of CM and DM in Smith chart for (a) case 3 and (b) case 4. Markers represent the self-resonance frequencies of CM and DM.

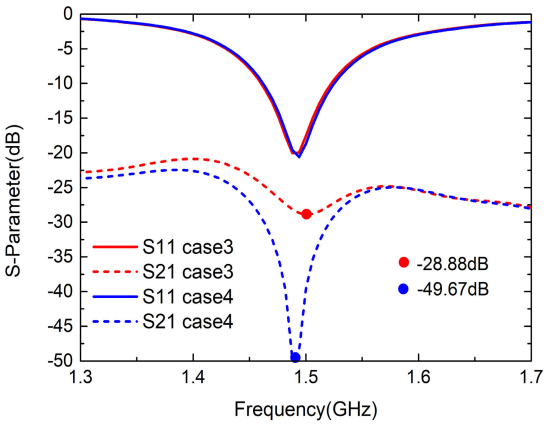

FIGURE 17. Comparison of S-parameters for case 3 and case 4.

(not shown) appears outside the frequency range of interest. Such a difference in the self-resonance frequencies of CM and DM leads to a larger value of RFD, which results in a worse isolation. The above phenomenon will be demonstrated through an example in Section IV (see Fig. 19 for details).

On the other hand, because for cases 2 and 3 there are two sets of the self-resonance frequencies of CM and DM, so as stated in Section II, one needs to calculate the RFD value for each set separately and take the average value as the final RFD value. The final values of RFD of case 2 and case 3 are1.90% and 0.64%, respectively. This of course shows that, among the three cases, case 3 offers the best decoupling effect; this was also proven in [26]. The above conclusion can certainly be verified by the results shown in Fig. 15.

Fig. 16(a) shows the impedances of the CM and DM in Smith chart for case 3. In order to further demonstrate the effectiveness of the proposed decoupling approach, a case where the antenna system has even better isolation effect [26] will be considered. It was shown in Fig. 15(a) of [26] that about 50dB isolation can be achieved if the value of Lg used in case 3 changes from 65mm to about 62.5mm; and for convenience we define this new case as case 4 (i.e., the size of the ground plane is: Wg = 80mm and Lg = 62.5mm). Fig. 16(b) shows the impedances of the CM and DM in Smith chart for case 4. Fig. 17 compares the S-parameters of case 3 and case 4. It can be seen from Fig. 17 that when the antenna structure is changed from case 3 to case 4, the isolation at the working frequency of this antenna system is improved from 28.88dB to 49.67dB. We will demonstrate that such an isolation improvement can also be predicted precisely with the proposed decoupling approach. To do so, the final values of RFD of case 3 and case 4 are calculated and compared. In particular, the calculated final RFD values for case 3 and case 4 are 0.64% and 0.4%, respectively; which just obeys the following rule: smaller RFD value leads to better decoupling effect. The above example certainly demonstrates that even this very precise decoupling effect can still be determined or evaluated by the proposed decoupling approach.

Form the above discussion, one can see that among the above three examples the decoupling condition proposed in [25]–[27] can only be easily applied to example 3, as can be seen from Fig. 16(b) the impedance curves of CM and DM in Smith chart are quite similar (or almost overlapped) for case 4 of example 3. For most antenna systems, however, the impedance curves of CM and DM in Smith chart look completely different (i.e., no obvious overlap). Nevertheless, the decoupling condition proposed in this article can be applied to any kind of symmetrical two-port antenna system.

IV. DISCUSSIONS

In this section, we will first show that the self-resonance frequency is the inherent characteristic of antennas. And, the decoupling effect can be evaluated only by comparing the self-resonance frequencies, rather than the resonance frequencies, of CM and DM. In order to demonstrate the characteristics of the proposed decoupling approach more clearly, some other related issues will also be discussed in this section.

First, as stated in Section II, the self-resonance frequency is the inherent frequency of an antenna system; and the self-resonance frequency can be obtained when the antenna system is excited by the normal antenna feeding port. The excitation port always contains a port resistance, R. Hence, in order to prove that the self-resonance frequency is the natural characteristic of an antenna, it is necessary to con-

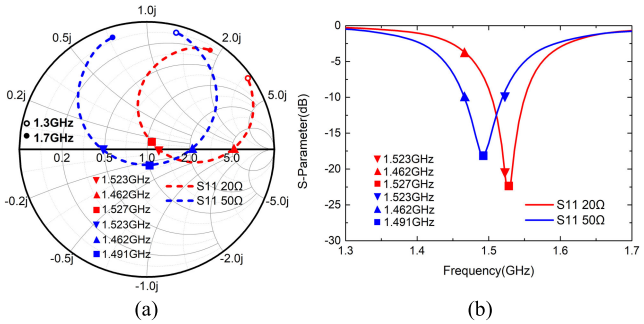

FIGURE 18. Simulated (a) Smith chart and (b) S11 of DM of case 3 of example 3. Markers represent both the self-resonance frequencies (solid triangles) and the resonance frequencies (solid squares) of DM.

firm that the obtained self-resonance frequency doesn't change with the port resistance. As an example, the DM of case 3 of example 3 is used for the above confirmation. Figs. 18(a) and 18(b) show respectively the impedances in Smith chart and S_{11} when the port is fed with two different resistances (50Ω and 20Ω); and the self-resonance frequencies and the resonance frequencies of the DM are represented by the solid triangles and squares, respectively. As expected, while R changes from 50Ω to 20Ω, the resonance frequency of the DM changes from 1.491 GHz to 1.527GHz. However, the two self-resonance frequencies (1.462 GHz and 1.523GHz) of the DM remain unchanged, as shown in Fig. 18. The above certainly confirms that the self-resonance frequency of an antenna can be obtained while it is excited by the normal antenna port. In order to be consistent with traditional calculations, however, it is recommended to use 50Ω as the port resistance.

Secondly, it has been pointed out in previous sections that when the RFD value is calculated, the self-resonance frequency, rather than the resonance frequency, of CM and DM should be used in Eq. (4). As an example, however, it can be seen from the results shown in Fig. 11(a) that the difference between the resonance frequencies of CM and DM is very similar to the difference between the self-resonance frequencies. Hence, when the optimal parameter is selected, two different judgment methods may lead to the same result. For instance, it can be seen from Fig. 11(a) that when either the self-resonance frequencies or the resonance frequencies of CM and DM are used to determine the optimal value of L_X, both give the same result: $L_X = 0.6$mm. However, it should be noted that it is not always correct to use the resonance frequencies of CM and DM to obtain the optimal parameter. To prove this, one of the variants of the two-dipole antenna system (i.e., example 1) is used as an example: except for the value of L_s changed from 20mm to 16mm, all the other parameters remain unchanged. The antenna performance of CM and DM in terms of S_{11} and Smith chart are shown in Figs. 19(a) and 19(b); and the S-parameter of the antenna system is illustrated in Fig. 19(c). It can be seen from Figs. 19 (a) and 19(b) that the resonance frequencies of CM and DM are 1.391GHz and 1.387GHz, respectively; whereas the self-resonance frequencies of CM and DM are 2.049GHz

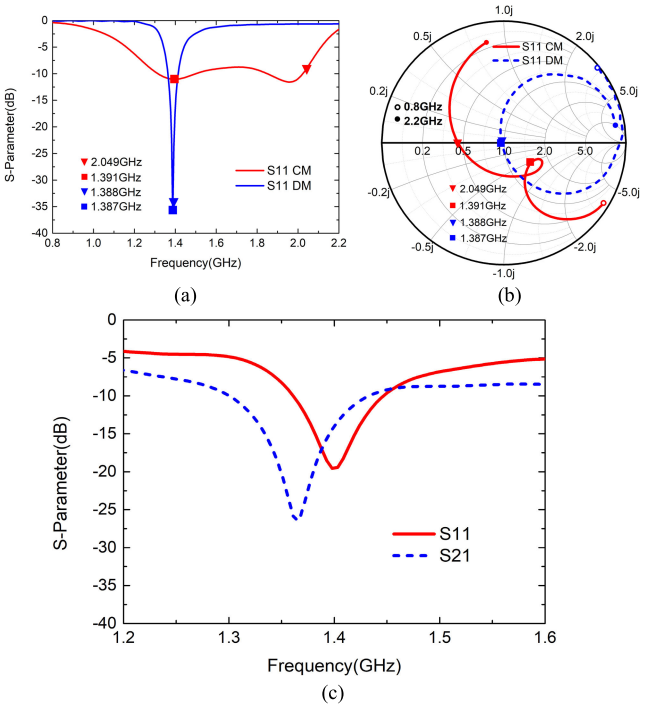

FIGURE 19. Comparison of CM and DM of two-dipole antenna system with Ls = 16mm (a) S11 and (b) Smith chart; and (c) S-parameter of the antenna system. Markers represent the self-resonance frequencies (solid triangles) and the resonance frequencies (solid squares) of CM and DM.

and 1.388GHz. Obviously, both the resonance frequencies of CM and DM are within the frequency range of interest (e.g., from 1.3-1.5GHz); however, the self-resonance frequencies of CM and DM are not. If the resonance frequencies of CM and DM are used, then the calculated RFD value is 0.29%. From this RFD data, one might conclude that very good isolation could be achieved. However, the results in Fig. 19(c) clearly illustrate that the decoupling effect is quite poor: the isolation at the resonance or working frequency (1.4GHz) is only about −14dB. This is mainly because the self-resonance frequency of CM (i.e., 2.049GHz) is outside the frequency range of interest. In fact, if the self-resonance frequencies of CM and DM are used to calculate the RFD value, this poor isolation behavior can still be predicated, as in this case the RFD value is as high as 38.46%. The above certainly demonstrates that optimal isolation cannot be obtained if the self-resonance frequencies of CM and DM are not simultaneously within the frequency range of interest.

The above discussion of course indicates that the resonance frequency of CM and DM cannot be used to evaluate the decoupling effect for the antenna systems considered in this article. However, it is always correct to use the self-resonance frequency of the CM and DM to evaluate the decoupling effect of any kind of symmetrical two-port antenna system. The above discussion definitely confirms the importance and accuracy of the proposed decoupling approach.

Thirdly, although the best decoupling effects can be achieved individually for the three examples used in this article, the degree of decoupling varies greatly. For example,

it can be seen from the decoupling results of example 1 (Fig. 4) and example 3 (Fig. 17) that the isolation bandwidth in example 3 is extremely wide, e.g., as can be seen from Fig. 17 that very good isolation effect can also be obtained outside the working frequency range of the antenna. However, the isolation bandwidth is relatively narrow in example 1. This is because, within the frequency range of interest, the CM and DM in example 1 have only one set of the self-resonant frequency; but there are two sets of the self-resonant frequencies in example 3. Having multiple self-resonant frequencies in the CM and DM will inevitably lead to good decoupling effect. This is because: the greater the number of antenna resonance frequencies, the larger the bandwidth.

V. CONCLUSION

In this article, a simple and effective antenna decoupling approach for a symmetrically and closely placed two-port antenna system is proposed. In particular, the approach is based on the coupling theory of the coupled resonant filter, and the extreme case (i.e., coupling coefficient = 0) of the coupled resonant filter is successfully applied to the antenna decoupling problem by using the CM and DM analysis. In addition, it is found that, for the first time, the antenna decoupling effect can be simply and easily evaluated by comparing the relative frequency difference of the self-resonance frequencies of CM and DM of antenna systems; and perfect antenna decoupling effect can be achieved when they are the same. The usefulness and effectiveness of the proposed decoupling approach have been verified and confirmed through several antenna examples.

On the other hand, the decoupling condition derived from the scattering parameter method [25]–[27] should satisfy the condition that the active S-parameters or the impedances of CM and DM in Smith chart are equal within the frequency range of interest. This also means that in order to know whether a good decoupling effect is achieved, the active S-parameters or the impedances of CM and DM in Smith chart must be compared within a certain range of frequency, not at a certain frequency. This makes the above judgement method suitable only for situations where the impedance curves of CM and DM in Smith chart are very similar or overlapped, as demonstrated in Sections III and IV. The above implies that the decoupling condition [25]–[27] can only be effectively applied to some special cases. However, the decoupling condition proposed in this article is based on the comparison of the self-resonance frequencies of CM and DM. Due to the above reasons, the proposed decoupling condition can be used as a general decoupling condition for any kind of two-port antenna system with a plane of symmetry. Moreover, although the proposed decoupling condition is still valid when the self-resonance frequencies of CM and DM are outside the frequency range of interest, the best isolation is achieved once both of them are within the frequency range of interest.

REFERENCES

[1] A. Diallo, C. Luxey, P. L. Thuc, R. Staraj, and G. Kossiavas, "Study and reduction of the mutual coupling between two mobile phone PIFAs operating in the DCS1800 and UMTS bands," *IEEE Trans. Antennas Propag.*, vol. 54, no. 11, pp. 3063–3074, Nov. 2006.
[2] Y. Wang and Z. Du, "A wideband printed dual-antenna with three neutralization lines for mobile terminals," *IEEE Trans. Antennas Propag.*, vol. 62, no. 3, pp. 1495–1500, Mar. 2014.
[3] K. L. Wong, J.-Y. Lu, L.-Y. Chen, W.-Y. Li, and Y.-L. Ban, "8-antenna and 16-antenna arrays using the quad-antenna linear array as a building block for the 3.5-GHz LTE MIMO operation in the smartphone," *Microw. Opt. Technol. Lett.*, vol. 58, no. 1, pp. 174–181, Jan. 2016.
[4] J. L. Guo, L. Cui, C. Li, and B. H. Sun, "Side-edge frame printed eight-port dual-band antenna array for 5G smartphone applications," *IEEE Trans. Antennas Propag.*, vol. 66, no. 12, pp. 7412–7417, Dec. 2018.
[5] M. Li, L. Jiang, and K. L. Yeung, "Novel and efficient parasitic decoupling network for closely coupled antennas," *IEEE Trans. Antennas Propag.*, vol. 67, no. 6, pp. 3574–3585, Jun. 2019.
[6] M. Li, L. Jiang, and K. L. Yeung, "A novel wideband decoupling network for two antennas based on the Wilkinson power divider," *IEEE Trans. Antennas Propag.*, vol. 68, no. 7, pp. 5082–5094, Jul. 2020.
[7] M. Li, J. M. Yasir, K. L. Yeung, and L. Jiang, "A novel dual-band decoupling technique," *IEEE Trans. Antennas Propag.*, vol. 68, no. 10, pp. 6923–6934, Oct. 2020.
[8] M.-Y. Li, Y. L. Ban, Z. Q. Xu, G. Wu, C. Y. D. Sim, K. Kang, and Z. F. Yu, "8-port orthogonally dual-polarized antenna array for 5G smartphone applications," *IEEE Trans. Antennas Propag.*, vol. 64, no. 9, pp. 3820–3830, Sep. 2016.
[9] M.-Y. Li, Z.-Q. Xu, Y.-L. Ban, C.-Y.-D. Sim, and Z.-F. Yu, "Eight-port orthogonally dual-polarized MIMO antennas using loop structures for 5G smartphone," *IET Microw., Antennas Propag.*, vol. 11, no. 12, pp. 1810–1816, Nov. 2017.
[10] C. Deng, Y. Li, X. Lv, and Z. Feng, "Wideband dual-mode patch antenna with compact CPW feeding network for pattern diversity application," *IEEE Trans. Antennas Propag.*, vol. 66, no. 5, pp. 2628–2633, May 2018.
[11] H. Xu, H. Zhou, S. Gao, H. Wang, and Y. Cheng, "Multimode decoupling technique with independent tuning characteristic for mobile terminals," *IEEE Trans. Antennas Propag.*, vol. 65, no. 12, pp. 6739–6751, Dec. 2017.
[12] J. Sui and K.-L. Wu, "Self-curing decoupling technique for two inverted-F antennas with capacitive loads," *IEEE Trans. Antennas Propag.*, vol. 66, no. 3, pp. 1093–1101, Mar. 2018.
[13] A. Zhao and Z. Ren, "Size reduction of self-isolated antenna MIMO antenna system for 5G mobile phone applications," *IEEE Antennas Wireless Propag. Lett.*, vol. 18, no. 1, pp. 152–156, Jan. 2019.
[14] J. Sui and K.-L. Wu, "A self-decoupled antenna array using inductive and capacitive couplings cancellation," *IEEE Trans. Antennas Propag.*, vol. 68, no. 7, pp. 5289–5296, Jul. 2020.
[15] Z. Ren, A. Zhao, and S. Wu, "MIMO antenna with compact decoupled antenna pairs for 5G mobile terminals," *IEEE Antennas Wireless Propag. Lett.*, vol. 18, no. 7, pp. 1367–1371, Jul. 2019.
[16] Z. Ren and A. Zhao, "Dual-band MIMO antenna with compact self-decoupled antenna pairs for 5G mobile applications," *IEEE Access*, vol. 7, pp. 82288–82296, 2019.
[17] X. Zhao, S. P. Yeo, and L. C. Ong, "Decoupling of inverted-F antennas with high-order modes of ground plane for 5G mobile MIMO platform," *IEEE Trans. Antennas Propag.*, vol. 66, no. 9, pp. 4485–4495, Jun. 2018.
[18] X. Tan, W. Wang, Y. Wu, Y. Liu, and A. A. Kishk, "Enhancing isolation in dual-band meander-line multiple antenna by employing split EBG structure," *IEEE Trans. Antennas Propag.*, vol. 67, no. 4, pp. 2769–2774, Apr. 2019.
[19] S. Zhang, S. Khan, and S. He, "Reducing mutual coupling for an extremely closely-packed tunable dual-element PIFA array through a resonant slot antenna formed in-between," *IEEE Trans. Antennas Propag.*, vol. 58, no. 8, pp. 2771–2776, Aug. 2010.
[20] S. Zhang, B. K. Lau, Y. Tan, Z. Ying, and S. He, "Mutual coupling reduction of two PIFAs with a T-shape slot impedance transformer for MIMO mobile terminals," *IEEE Trans. Antennas Propag.*, vol. 60, no. 3, pp. 1521–1531, Mar. 2012.
[21] B. Qian, X. Chen, and A. Kishk, "Decoupling of microstrip antennas with defected ground structure using the common/differential mode theory," *IEEE Antennas Wireless Propag. Lett.*, vol. 20, no. 5, pp. 828–832, May 2021.

[22] C.-D. Xue, X. Y. Zhang, Y. F. Cao, Z. Hou, and C. F. Ding, "MIMO antenna using hybrid electric and magnetic coupling for isolation enhancement," *IEEE Trans. Antennas Propag.*, vol. 65, pp. 5162–5170, Oct. 2017.
[23] F. Liu, J. Guo, L. Zhao, G.-L. Huang, Y. Li, and Y. Yin, "Dual-band metasurface-based decoupling method for two closely packed dual-band antennas," *IEEE Trans. Antennas Propag.*, vol. 68, no. 1, pp. 552–557, Jan. 2020.
[24] H. Xu, S. Gao, H. Zhou, H. Wang, and Y. Cheng, "A highly integrated MIMO antenna unit: Differential/common mode design," *IEEE Trans. Antennas Propag.*, vol. 67, no. 11, pp. 6724–6734, Nov. 2019.
[25] L. Sun, Y. Li, Z. Zhang, and H. Wang, "Self-decoupled MIMO antenna pair with shared radiator for 5G smartphones," *IEEE Trans. Antennas Propag.*, vol. 68, no. 5, pp. 3423–3432, May 2020.
[26] L. Sun, Y. Li, Z. Zhang, and H. Wang, "Antenna decoupling by common and differential modes cancellation," *IEEE Trans. Antennas Propag.*, vol. 69, no. 2, pp. 672–682, Feb. 2021.
[27] L. Sun, Y. Li, and Z. Zhang, "Decoupling between extremely closely spaced patch antennas by mode cancellation method," *IEEE Trans. Antennas Propag.*, vol. 69, no. 6, pp. 3074–3083, Jun. 2021.
[28] J.-S. Hong and M. J. Lancaster, "Couplings of microstrip square open-loop resonators for cross-coupled planar microwave filters," *IEEE Trans. Microw. Theory*, vol. 44, no. 11, pp. 2099–2109, Nov. 1996.
[29] J.-S. Hong, *Microstrip Filters for RF/Microwave Applications*. Hoboken, NJ, USA: Wiley, 2011.
[30] Q.-X. Chu and H. Wang, "A compact open-loop filter with mixed electric and magnetic coupling," *IEEE Trans. Microw. Theory Techn.*, vol. 56, no. 2, pp. 431–439, Feb. 2008.
[31] X. Yan, J. C. Gore, and W. A. Grissom, "Self-decoupled radiofrequency coils for magnetic resonance imaging," *Nature Commun.*, vol. 9, no. 1, Aug. 2018, Art. no. 3481.
[32] D. E. Bockelman and W. R. Eisenstadt, "Combined differential and common-mode scattering parameters: Theory and simulation," *IEEE Trans. Microw. Theory Techn.*, vol. 43, no. 7, pp. 1530–1539, Jul. 1995.

ANPING ZHAO (Senior Member, IEEE) received the B.Sc. degree in optical physics from the Changchun University of Science and Technology, China, in 1984, the M.Sc. degree in optics from the Changchun Institute of Physics, Chinese Academy of Sciences, China, in 1987, and the Ph.D. degree in electronic and electrical engineering from Brunel University, Brunel, U.K., in 1994.

From 1987 to 1989, he was a Researcher at the Changchun Institute of Physics. In January 1990, he joined the Department of Electronic and Electrical Engineering, Surrey University, Surrey, U.K., as a Visiting Research Fellow, where he was involved on the computer verification of optical waveguide characteristics based on multiple-quantum-well (MWQ) structures in III-V semiconductor materials. In September 1994, he joined the Radio Laboratory, Department of Electrical and Communications Engineering, Helsinki University of Technology, Helsinki, Finland, where he was involved on the computer-aided-design of microwave and millimeter-wave circuits with the FDTD method. He joined Nokia Research Center, Helsinki, in October 1997. From October 1997 to August 2007, he was a Senior Research Engineer/Principal Researcher with Nokia Research Centre. From September 2007 to September 2012, he was a Principal Scientist with Nokia Research Center, Beijing, China. In October 2012, he joined Shenzhen Sunway Communication Company Ltd., working as a Chief Technical Expert and the Director of Advanced Antenna Technology Department of the Sunway Central Research Institute. Since July 2019, he has been working as a Chief Antenna Expert at Huami Information and Technology Company Ltd., Shenzhen. He has authored more than 130 refereed articles and holds about 40 granted invention patents. His current research interests include antenna designs for 4G LTE, MIMO antenna system and millimeter-wave antenna designs for 5G applications, and other antennas used in portable devices. He is listed in Marquis Who's Who in the World and Who's Who in Sciences and Engineering.

ZHOUYOU REN (Member, IEEE) received the B.Sc. degree in communication engineering from Beijing Jiaotong University, Beijing, China, in 2014, and the M.Sc. degree in data communication from The University of Sheffield, U.K., in 2016. In 2017, he joined Shenzhen Sunway Communication Company Ltd., as a RF Engineer, and became a Senior RF Engineer, in 2019. He is currently with Huami Information Technology Company Ltd., Shenzhen, China, as a Senior Antenna Engineer of the Global Innovation Center for Emerging Wearables, Healthcare equipment. He holds over 20 granted U.S./CN patents. His current research interests include antenna decoupling techniques and millimeter-wave antennas, and MIMO antenna systems for 5G applications. He has served as a Reviewer for IEEE Access, *Journal of Electromagnetic Waves and Applications*, and *International Journal of Microwave and Wireless Technologies*.